ASM Sci. J., Special Issue 6, 2019 for SKSM26, 179-185

Lower Stagnation Point Flow of Jeffrey Nanofluid on a Sphere with Mixed Convection

Syazwani MohdZokri*, Nur Syamilah Arifin, Abdul Rahman Mohd Kasim and Mohd Zuki Salleh

[1]*Faculty of Industrial Sciences & Technology, Universiti Malaysia Pahang, 26300 UMP Kuantan, Pahang, Malaysia*

A theoretical analysis for Jeffrey nanofluid flow induced by a sphere with mixed convection near lower stagnation point flow is deliberated. Formulation of the basic governing equations is according to the Buongiorno model. The dimensional highly nonlinear equations are first converted into non-dimensional form with the assistance of non-dimensional variables. The complexity of the resulting equations is subsequently reduced using the appropriate non-similarity transformation variables. Numerical solution is generated via the Runge-KuttaFehlberg method (RKF 45) to probe into the impacts of Jeffrey fluid and nanofluid parameters on the specified distributions. Findings have shown that the increase of Deborah number has decelerated the fluid flow and enhanced the temperature. The mixed convection parameter has escalated the fluid flow, whereas the temperature performs oppositely. Besides, a rise in thermophoresis diffusion parameter has declined and escalated the Nusselt and Sherwood numbers, respectively.

Keywords: Jeffrey nanofluid; sphere; lower stagnation point flow; mixed convection

I. INTRODUCTION

Studies on the non-Newtonian transport phenomena have acquired exceptional attention from the researchers and engineers owing to their countless applications in various branches of process mechanical, chemical and materials engineering. A number of suggested non-Newtonian fluid models possessing disparate fluid features has been highlighted in the literature including micropolar fluid (Salleh *et al.*, 2010a), Casson fluid (Arifin *et al.*, 2017), viscoelastic fluid (Kasim *et al.*, 2013), Maxwell fluid (Halim *et al.*, 2017), Jeffrey fluid (Zokri *et al.*, 2018) and many more. Of all, the most common and simplest model of non-Newtonian fluid known as viscoelastic Jeffrey fluid model is favored essentially because of its capacity in expressing the dual features of retardation and relaxation.

Nonetheless, there exists a great concern over the poor thermal conductivity of the Jeffrey fluid model. A modern science technique named nanofluid was principally familiarized by Choi (1995) to express the dispersion of nanometer-sized particles with dimension less than 100 nm in the conventional fluids. This fluid has also been regarded as one of the contemporary research areas by reason of its remarkable potential in enhancing heat transfer as well as having great potential for heat exchange rate (Tham *et al.*, 2013). Some latest works relating to the suspension of nanoparticles in the conventional fluids can be retrieved in (Zokri *et al.*, 2017; Ibrahim *et al.*, 2017; Hsiao, 2017; Hayat *et al.*, 2018; Usman *et al.*, 2018).

Flow past a sphere with mixed convection was first considered experimentally by Yuge (1960). The analytical and experimental studies were then continued by Hieber and Gebhart (1969) to incorporate the impact of a very small local Grash of and Reynolds numbers. Then, the flow of viscous and micropolar fluid was discussed by Nazar *et al.* (2002a; 2002b; 2003a; 2003b) from a sphere and heated under the constant surface temperature and heat flux.A detailed discussion on the influence of mixed convection parameter was thoroughly explored together with the separation of boundary layer. In view of similar

*Corresponding author's e-mail: zuki@ump.edu.my

problem, the joint impact of free and forced convection from a solid sphere was examined by Salleh *et al.* (2010a; 2010b)in the respective viscous and micropolar fluid with Newtonian heating condition. Similarly, the combined convection induced by a sphere was studied by Tham *et al.* (2013) in nanofluid with gyrotactic microorganisms. Aziz *et al.* (2017) scrutinized the consequence of magnetohydrodynamic effect in viscoelastic micropolar fluid passing through a sphere.

In all of the above study, it is apparent that the Jeffrey nanofluid model past a sphere has yet to be deliberated near the lower stagnation region. Therefore, the current study aims at exploring the flow of Jeffrey nanofluid from a sphere with mixed convection at the lower stagnation point. In detail, mixed convection refers to the amalgamation of the free and forced convections. The mixed convection impact can be determined by the buoyancy parameter, $\gamma = \frac{Gr_x}{\mathrm{Re}_x^n}$, where Gr_x, Re_x and n are defined as the respective local Grash of number, local Reynolds number and a positive constant. According to Pop and Ingham (2001) and Kreith *et al.* (2012), the forced convection dominates when $\gamma \to 0,$ but free convection dominates when $\gamma \to \infty.$

II. MATHEMATICAL FORMULATION

Suppose two dimensional Jeffrey nanofluid flow from a sphere of radius a in the $\bar{x}-\bar{y}$ plane near the lower stagnation region, $\bar{x} \approx 0$ is considered as exemplified in Figure 1.

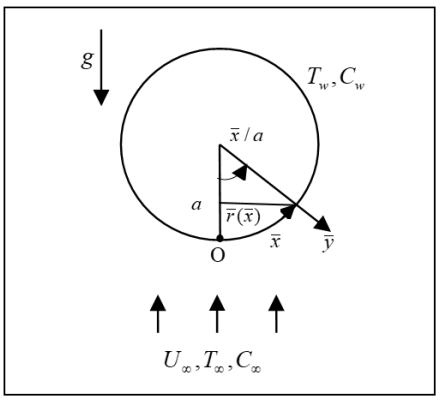

Figure 1 Schematic diagram of the problem

From Figure 1, the $\bar{x}$ and $\bar{y}$ axes are taken in such a way that it determines the distance along the sphere surface and perpendicular to it, respectively. The direction of gravity acceleration, g is oriented downwards. Further, T_w, T_∞, C_w and C_∞ be the surface temperature, ambient temperature, surface concentration and ambient concentration. The basic governing equations describing the situations are:

$$\frac{\partial}{\partial \bar{x}}\left(\bar{r}\ \bar{u}\right)+\frac{\partial}{\partial \bar{y}}\left(\bar{r}\ \bar{v}\right)=0, \tag{1}$$

$$\bar{u}\frac{\partial \bar{u}}{\partial \bar{x}}+\bar{v}\frac{\partial \bar{u}}{\partial \bar{y}}=\bar{u}_e\frac{d\bar{u}_e}{d\bar{x}}+\frac{\nu}{1+\lambda}\left[\frac{\partial^2 \bar{u}}{\partial \bar{y}^2}+\lambda_1\left(\bar{u}\frac{\partial^3 \bar{u}}{\partial \bar{x}\partial \bar{y}^2}-\frac{\partial \bar{u}}{\partial \bar{x}}\frac{\partial^2 \bar{u}}{\partial \bar{y}^2}+\bar{v}\frac{\partial^3 \bar{u}}{\partial \bar{y}^3}+\frac{\partial \bar{u}}{\partial \bar{y}}\frac{\partial^2 \bar{u}}{\partial \bar{x}\partial \bar{y}}\right)\right]+ g\beta_T(T-T_\infty)\sin\frac{\bar{x}}{a}+g\beta_C(C-C_\infty)\sin\frac{\bar{x}}{a}, \tag{2}$$

$$\bar{u}\frac{\partial T}{\partial \bar{x}}+\bar{v}\frac{\partial T}{\partial \bar{y}}=\alpha\frac{\partial^2 T}{\partial \bar{y}^2}+\tau\left[D_B\frac{\partial C}{\partial \bar{y}}\frac{\partial T}{\partial \bar{y}}+\frac{D_T}{T_\infty}\left(\frac{\partial T}{\partial \bar{y}}\right)^2\right] \tag{3}$$

$$\bar{u}\frac{\partial C}{\partial \bar{x}}+\bar{v}\frac{\partial C}{\partial \bar{y}}=D_B\frac{\partial^2 C}{\partial \bar{y}^2}+\frac{D_T}{T_\infty}\frac{\partial^2 T}{\partial \bar{y}^2} \tag{4}$$

where $\bar{u}$ and $\bar{v}$ are the respective velocity components along the $\bar{x}$ and $\bar{y}$ directions. The associated boundary conditions are

$$\begin{aligned} &\bar{u}(\bar{x},0)=0,\ \bar{v}(\bar{x},0)=0,\\ &T(\bar{x},0)=T_w,\ C(\bar{x},0)=C_w \qquad \text{at } \bar{y}=0\\ &\bar{u}(\bar{x},\infty)\to\bar{u}_e,\ \bar{v}(\bar{x},\infty)\to 0,\\ &T(\bar{x},\infty)\to T_\infty,\ C(\bar{x},\infty)\to C_\infty \qquad \text{as } \bar{y}\to\infty \end{aligned} \tag{5}$$

In the above equations, the respective local free stream velocity, ratio of heat capacity of the nanoparticle to the fluid and radial distance from the symmetrical axis to the sphere surface are symbolized as $\bar{u}_e$, τ and $\bar{r}(\bar{x}),$ and can be expressed as follows

$$\bar{u}_e(\bar{x})=\frac{3}{2}U_\infty\sin\left(\frac{\bar{x}}{a}\right),\ \tau=(\rho c)_p/(\rho c)_f,\ \bar{r}(\bar{x})=a\sin\left(\frac{\bar{x}}{a}\right) \tag{6}$$

Furthermore, C, C_p, D_B, D_T, Pr, T, β_T, β_C, ν, α, ρ, μ, λ, λ_1 and k are the local concentration, specific heat capacity, Brownian diffusion coefficient, thermophoretic diffusion coefficient,Prandtl number, local temperature, thermal expansion, concentration expansion, kinematic viscosity, thermal diffusivity, density, dynamic viscosity, ratio of relaxation to retardation times, retardation time and thermal conductivity. Initiating the succeeding non-dimensional variables:

$$r=\frac{\bar{r}}{a},\ x=\frac{\bar{x}}{a},\ y=\frac{\mathrm{Re}^{1/2}\,\bar{y}}{a},\ u=\frac{\bar{u}}{U_\infty},$$
$$v=\frac{\mathrm{Re}^{1/2}\,\bar{v}}{U_\infty},\ u_e(x)=\frac{\bar{u}_e(x)}{U_\infty}, \tag{7}$$
$$\theta(\eta)=\frac{T-T_\infty}{T_w-T_\infty},\ \phi(\eta)=\frac{C-C_\infty}{C_w-C_\infty}$$

Then, using Eq. (7), Eqs. (1) to (4) give rise to the ensuing dimensionless form of partial differential equations:

$$\frac{\partial}{\partial x}(ru)+\frac{\partial}{\partial y}(rv)=0 \tag{8}$$

$$u\frac{\partial u}{\partial x}+v\frac{\partial u}{\partial y}=u_e\frac{du_e}{dx}+\frac{1}{1+\lambda}\left[\begin{array}{l}\dfrac{\partial^2 u}{\partial y^2}+\\ \lambda_2\left(u\dfrac{\partial^3 u}{\partial x\partial y^2}-\dfrac{\partial u}{\partial x}\dfrac{\partial^2 u}{\partial y^2}+v\dfrac{\partial^3 u}{\partial y^3}+\dfrac{\partial u}{\partial y}\dfrac{\partial^2 u}{\partial x\partial y}\right)\end{array}\right]+\gamma\left[\theta+N\phi\right]\sin x \tag{9}$$

$$u\frac{\partial\theta}{\partial x}+v\frac{\partial\theta}{\partial y}=\frac{1}{\mathrm{Pr}}\frac{\partial^2\theta}{\partial y^2}+Nb\frac{\partial\phi}{\partial y}\frac{\partial\theta}{\partial y}+Nt\left(\frac{\partial\theta}{\partial y}\right)^2 \tag{10}$$

$$u\frac{\partial\phi}{\partial x}+v\frac{\partial\phi}{\partial y}=\frac{1}{Le\,\mathrm{Pr}}\left(\frac{\partial^2\phi}{\partial y^2}+\frac{Nt}{Nb}\frac{\partial^2\theta}{\partial y^2}\right) \tag{11}$$

where λ_2, γ, Gr, Re, N, Nb, Nt and Le denote the Deborah number, mixed convection parameter, Grash of number, Reynolds number, concentration buoyancy parameter, Brownian motion, thermophoresis diffusion parameter and Lewis number, and are given as

$$\mathrm{Pr}=\frac{\nu}{\alpha},\ \lambda_2=\frac{\lambda_1 U_\infty}{a},\ \gamma=\frac{Gr}{\mathrm{Re}_x^2},\ Gr=\frac{a^3 g\beta_T\left(T_w-T_\infty\right)}{v^2}$$
$$\mathrm{Re}=\frac{U_\infty a}{v},\ N=\frac{\beta_C\left(C_w-C_\infty\right)}{\beta_T\left(T_w-T_\infty\right)},\ Nb=\frac{\tau D_B(C_w-C_\infty)}{\nu}$$
$$Le=\frac{\alpha}{D_B},\ Nt=\frac{\tau D_T(T_w-T_\infty)}{\nu T_\infty}$$

The corresponding boundary conditions are

$$\begin{array}{l}u(x,0)=0,\quad v(x,0)=0,\\ \theta(x,0)=1,\quad \phi(x,0)=1 \qquad \text{at}\ \ y=0\\ u(x,\infty)\to u_e,\quad v(x,\infty)\to 0,\\ \theta(x,\infty)\to 0,\quad \phi(x,\infty)\to 0\ \text{ as }\ y\to\infty\end{array} \tag{12}$$

Introducing the stream function ψ, which is denoted as follows

$$u=\frac{1}{r}\frac{\partial\psi}{\partial y}\ \text{and}\ v=-\frac{1}{r}\frac{\partial\psi}{\partial x} \tag{13}$$

When $x\to 0$, then $\sin x/x\to 1$. Therefore, it is suitable to inaugurate the subsequent non-similarity transformation variables

$$\psi=xr(x)f(x,y),\ \theta=\theta(x,y),\ \phi=\phi(x,y), \tag{14}$$

Now, the satisfaction of Eq. (8) is unavoidable and Eqs. (9) to (12) become

$$\begin{array}{l}\dfrac{1}{1+\lambda}f'''-\left(f'\right)^2+\dfrac{\sin x}{x}\left[\gamma\left(\theta+N\phi\right)\right]+\\ +\dfrac{\lambda_2}{1+\lambda}\left[\left(f''\right)^2-\left(1+\dfrac{x}{\sin x}\cos x\right)ff^{(iv)}\right]\\ +\left(1+\dfrac{x}{\sin x}\cos x\right)ff''+\dfrac{9}{4}\dfrac{\sin x\cos x}{x}=\\ x\left[\begin{array}{l}f'\dfrac{\partial f'}{\partial x}-f''\dfrac{\partial f}{\partial x}+\dfrac{\lambda_2}{1+\lambda}\\ \left(f'''\dfrac{\partial f'}{\partial x}+f^{(iv)}\dfrac{\partial f}{\partial x}-f''\dfrac{\partial f''}{\partial x}-f'\dfrac{\partial f'''}{\partial x}\right)\end{array}\right]\end{array} \tag{15}$$

$$\begin{array}{l}\dfrac{1}{\mathrm{Pr}}\theta''+\left(1+\dfrac{x}{\sin x}\cos x\right)f\theta'+Nb\theta'\phi'+\\ Nt\left(\theta'\right)^2=x\left[f'\dfrac{\partial\theta}{\partial x}-\theta'\dfrac{\partial f}{\partial x}\right]\end{array} \tag{16}$$

$$\begin{array}{l}\phi''+\dfrac{Nt}{Nb}\theta''+\left(1+\dfrac{x}{\sin x}\cos x\right)Le\,\mathrm{Pr}\,f\phi'=\\ xLe\,\mathrm{Pr}\left[f'\dfrac{\partial\phi}{\partial x}-\phi'\dfrac{\partial f}{\partial x}\right]\end{array} \tag{17}$$

$$\begin{array}{l}f(x,0)=0,\ f'(x,0)=0,\\ \theta(x,0)=1,\ \phi(x,0)=1 \qquad \text{at}\ \ y=0\\ f'(x,\infty)\to\dfrac{3}{2}\dfrac{\sin x}{x},\ f''(x,\infty)\to 0,\\ \theta(x,\infty)\to 0,\ \phi(x,\infty)\to 0\ \text{ as }\ y\to\infty\end{array} \tag{18}$$

Interestingly, when $x \approx 0$, Eqs. (15) to (17) with boundary conditions (18) are reduced to the succeeding ordinary differential equations

$$\frac{1}{1+\lambda}\left[f''' + \lambda_2\left((f'')^2 - 2ff^{(iv)}\right)\right] - (f')^2 + 2ff'' + \gamma(\theta + N\phi) + \frac{9}{4} = 0, \tag{19}$$

$$\frac{1}{\Pr}\theta'' + 2f\theta' + Nb\theta'\phi' + Nt(\theta')^2 = 0 \tag{20}$$

$$\phi'' + \frac{Nt}{Nb}\theta'' + 2Le\Pr f\phi' = 0 \tag{21}$$

$$f(0) = 0,\ f'(0) = 0,\ \theta(0) = 1,\ \phi(0) = 1$$
$$f'(\infty) \to \frac{3}{2},\ f''(\infty) \to 0,\ \theta(\infty) \to 0,\ \phi(\infty) \to 0 \tag{22}$$

The respective skin friction coefficient, Nusselt number and Sherwood number are denoted as C_f, Nu_x and Sh_x, and given by

$$C_f = \frac{\tau_w}{\rho_f U_\infty^2},\ Nu_x = \frac{aq_w}{k_f(T_w - T_\infty)},$$
$$Sh_x = \frac{aj_p}{D_B(C_w - C_\infty)} \tag{23}$$

where τ_w, q_w and j_p are the respective surface shear stress, heat and mass fluxes, which are given by

$$\tau_w = \frac{\mu}{1+\lambda}\left[\frac{\partial \bar{u}}{\partial \bar{y}} + \lambda_1\left(\bar{u}\frac{\partial^2 \bar{u}}{\partial \bar{x}\partial \bar{y}} + \bar{v}\frac{\partial^2 \bar{u}}{\partial \bar{y}^2}\right)\right]_{\bar{y}=0},$$
$$q_w = -k_f\left(\frac{\partial T}{\partial \bar{y}}\right)_{\bar{y}=0},\ j_p = -D_B\left(\frac{\partial C}{\partial \bar{y}}\right)_{\bar{y}=0}$$

The dimensionless form of skin friction coefficient, Nusselt number and Sherwood number are as the following upon applying Eqs. (7) and (14)

$$C_f \operatorname{Re}_x^{1/2} = \frac{xf''(x,0)}{1+\lambda},\ Nu_x \operatorname{Re}_x^{-1/2} = -\theta'(x,0),$$
$$Sh_x \operatorname{Re}_x^{-1/2} = -\phi'(x,0) \tag{24}$$

III. RESULTS AND DISCUSSIONS

Comprehensive numerical solutions are engaged graphically to reveal the impacts of three pertinent parameters, comprising of the mixed convection parameter γ, Deborah number λ_2 and Brownian motion Nb. These solutions are acquired via the Runge-KuttaFehlberg method (RKF 45) by employing the highly nonlinear equations (19) to (21) with boundary conditions (22). All parameters utilized in this endeavor are fixed to be as follows, otherwise specified: $\lambda = 0.1,\ \lambda_2 = \gamma = 0.2,$ $Nb = Nt = N = 0.3,\ Le = 10$ and $\Pr = 1$. Validation of the computational results generated throughout this study is conducted by way of comparison as accessible in Table 1. The reported results obtained via the Keller-box method by two different authors, namely Nazar *et al.* (2003b)and Salleh *et al.* (2010b)for different values of $-\theta'(0)$ are taken into consideration, and are found to be in an excellent consistency with that of the present ones. Such outcome has guaranteed the proficiency of the implemented method, thus assuring the accuracy of the current results. Furthermore, it is worth pointing out that when $\lambda = \lambda_2 = \gamma = 0,$ the boundary layer equations (19) to (21) come to be decoupled. In view of that, evidently, the skin friction coefficient for dissimilar $\Pr$ values result in a unique solution, $f''(0) = 2.410183,$ which is in line with the solutions reported by Nazar *et al.* (2002a; 2002b; 2003b) $(f''(0) = 2.4151)$ and Salleh *et al.* (2010a) $(f''(0) = 2.4104).$

Illustration of the graphical outcomes for profiles of velocity, temperature, Nusselt number and Sherwood number are exhibited through Figures 2 to 7 for several values of γ, λ_2, Nb and Nt. From Figures 2 and 3, it is obvious that γ has an opposite effect on the fluid flow and temperature. A large value of γ enhances the buoyancy force effect that triggers a favorable pressure gradient. Such situation is liable to the escalation of the fluid motion and reduction of the temperature.

Figure 4 and 5 demonstrate the impact of λ_2 on the velocity and temperature profiles. The fluid flow is significantly reduced, but the temperature acts contrarily as λ_2 upsurges. Physically, λ_2 is basically an amalgamation of both viscous and elastic behaviors that capable to determine the viscoelasticity property of the materials. A

greater viscoelasticity property promotes the frictional force whilst slows down the fluid flow. Also, extra heat ensuing from the frictional force has consequently improved the temperature. Accordingly, the decline in the velocity and the rise in the temperature are predictable.

Figure 6 and 7 are sketched to inspect the outcome of Nb and Nt towards the $Nu_x \operatorname{Re}_x^{-1/2}$ and $Sh_x \operatorname{Re}_x^{-1/2}$. A rise of both Nb and Nt gives rise to the reduction of the $Nu_x \operatorname{Re}_x^{-1/2}$, whereas the $Sh_x \operatorname{Re}_x^{-1/2}$ reflects a contradict behaviour. The reason is that increasing Nb tends to stimulate the collision amongst the particles of fluid and their arbitrary motions. This collision generates extra heat, which consequently deteriorates the heat transfer whilst augments the nanoparticles concentration transfer.

Table 1. Comparative values of $-\theta'(0)$ with existing publications for different values of γ when $\lambda = \lambda_2 = Nb = Nt = N = Le = 0$ and $Pr = 0.7$

γ	Nazar *et al.* (2003b)	Salleh *et al.* (2010b)	Present
-4.6	0.6011	0.5990	0.600969
-4.5	0.6117	0.6115	0.611401
-4.0	0.6534	0.6528	0.652717
-3.0	0.7108	0.7099	0.709826
-2.0	0.7529	0.7519	0.751819
-1.0	0.7870	0.7860	0.785927
-0.5	0.8021	0.8010	0.800994
0.0	0.8162	0.8150	0.815036
1.0	0.8463	0.8406	0.840637
2.0	0.8648	0.8636	0.863614
3.0	0.8857	0.8845	0.884539
4.0	0.9050	0.9038	0.903807
5.0	0.9230	0.9217	0.921705
6.0	0.9397	0.9385	0.938445
7.0	0.9555	0.9542	0.954198
8.0	0.9704	0.9691	0.969089
9.0	0.9846	0.9833	0.983225
10.0	0.9981	0.9967	0.996692
20.0	1.1077	1.1061	1.106049

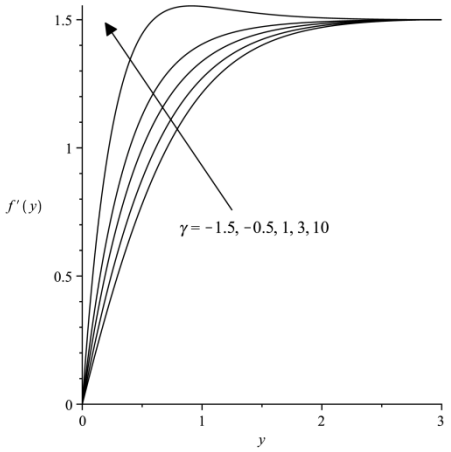

Figure 2. $f'(y)$ for varied values of γ

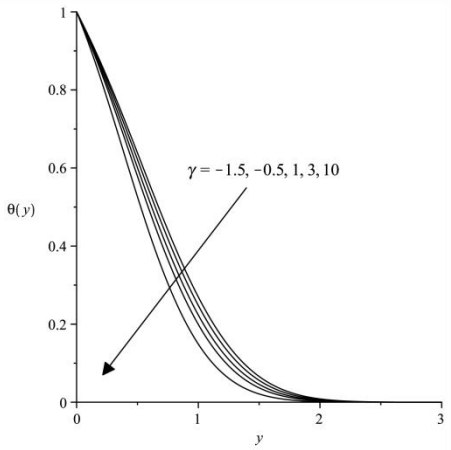

Figure 3. $\theta(y)$ for varied values of γ

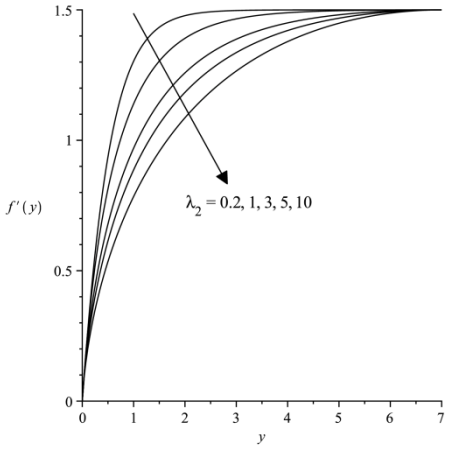

Figure 4. $f'(y)$ for varied values of λ_2

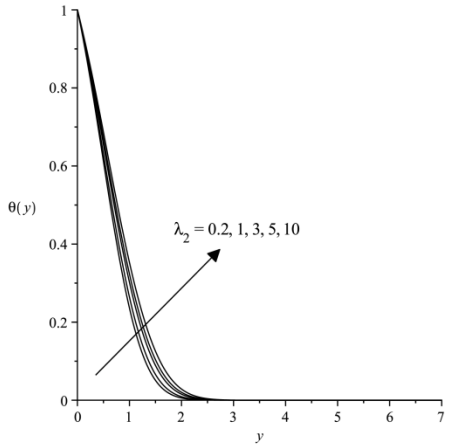

Figure 5. $\theta(y)$ for varied values of λ_2

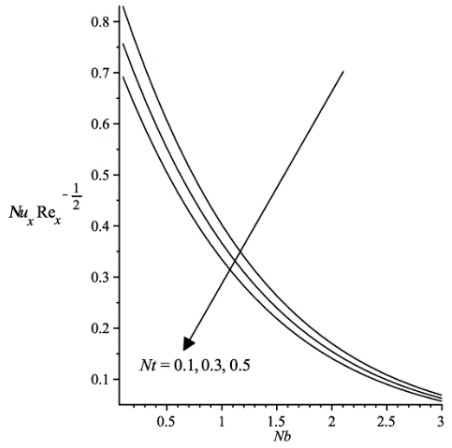

Figure 6. $Nu_x \, \mathrm{Re}_x^{-1/2}$ for varied values of Nb and Nt

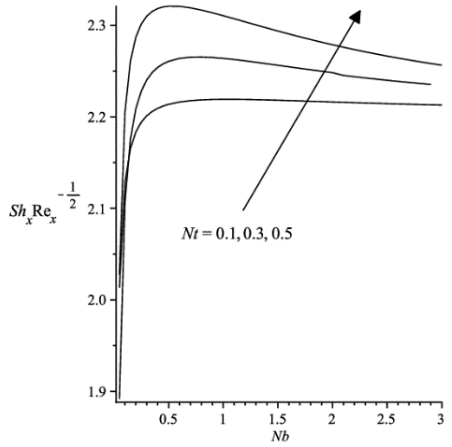

Figure 7. $Sh_x \, \mathrm{Re}_x^{-1/2}$ for varied values of Nb and Nt

IV. CONCLUSION

This study has generally presented the Jeffrey nanofluid flow towards a sphere near the lower stagnation region with mixed convection. The following general conclusions can be deduced from this investigation:

- Parameter γ is the accelerating function of velocity but declining function of temperature.
- Parameter λ_2 has lessened the velocity but heightened the temperature.
- Parameter Nb has augmented the velocity and diminished the temperature.

V. ACKNOWLEDGEMENT

The authors acknowledge the provision received from the Universiti Malaysia Pahang (UMP) via research grants PGRS1703100,RDU1703258 and RDU170358.

VI. ACKNOWLEDGEMENT

Arifin, N. S., Zokri, S. M., Kasim, A. R. M., Salleh, M. Z., Yusoff, W. N. S. W., Mohammad, N. F. & Shafie, S. (2017). Aligned magnetic field on dusty Casson fluid over a stretching sheet with Newtonian heating. Malaysian Journal of Fundamental and Applied Sciences. 13, 245-248.

Aziz, L. A., Kasim, A. R. M., Salleh, M. Z., Yusoff, N. S. & Shafie, S. (2017). Magnetohydrodynamics effect on convective boundary layer flow and heat transfer of viscoelastic micropolar fluid past a sphere. Journal of Physics: Conference Series. 890, 012003.

Choi, S. U. S. (1995). Enhancing thermal conductivity of fluids with nanoparticles. 1995 International mechanical engineering congress and exhibition. San Francisco, United States. 12-17 Nov 1995, 99-105.

Halim, N. A., Haq, R. U. & Noor, N. F. M. (2017). Active and passive controls of nanoparticles in Maxwell stagnation point flow over a slipped stretched surface. Meccanica. 52, 1527-1539.

Hayat, T., Kiyani, M. Z., Alsaedi, A., Khan, M. I. & Ahmad, I. (2018). Mixed convective three-dimensional flow of Williamson nanofluid subject to chemical reaction. International Journal of Heat and Mass Transfer. 127, 422-429.

Hieber, C. A. & Gebhart, B. (1969). Mixed convection from a sphere at small Reynolds and Grashof numbers. Journal of Fluid Mechanics. 38, 137-159.

Hsiao, K.-L. (2017). Micropolar nanofluid flow with MHD and viscous dissipation effects towards a stretching sheet with multimedia feature. International Journal of Heat and Mass Transfer. 112, 983-990.

Ibrahim, S. M., Lorenzini, G., Kumar, P. V. & Raju, C. S. K. (2017). Influence of chemical reaction and heat source on dissipative MHD mixed convection flow of a Casson nanofluid over a nonlinear permeable stretching sheet. International Journal of Heat and Mass Transfer. 111, 346-355.

Kasim, A. R. M., Mohammad, N. F., Shafie, S. & Pop, I. (2013). Constant heat flux solution for mixed convection boundary layer viscoelastic fluid. Heat and Mass Transfer. 49, 163-171.

Kreith, F., Manglik, R. M. & Bohn, M. S. (2012). Principles of heat transfer: Cengage Learning.

Nazar, R., Amin, N. & Pop, I. (2002a). Mixed convection boundary layer flow from a sphere with a constant surface heat flux in a micropolar fluid. Journal of Energy Heat and Mass Transfer. 24, 195-212.

Nazar, R., Amin, N. & Pop, I. (2002b). On the mixed convection boundary-layer flow about a solid sphere with constant surface temperature. Arabian Journal for Science and Engineering. 27, 117-135.

Nazar, R., Amin, N. & Pop, I. (2003a). Mixed convection boundary-layer flow from a horizontal circular cylinder in micropolar fluids: case of constant wall temperature. International Journal of Numerical Methods for Heat & Fluid Flow. 13, 86-109.

Nazar, R., Amin, N. & Pop, I. (2003b). Mixed convection boundary layer flow about an isothermal sphere in a micropolar fluid. International Journal of Thermal Sciences. 42, 283-293.

Pop, I. & Ingham, D. B. (2001). Convective heat transfer: mathematical and computational modelling of viscous fluids and porous media: Elsevier.

Salleh, M. Z., Nazar, R. & Pop, I. (2010a). Mixed convection boundary layer flow from a solid sphere with Newtonian heating in a micropolar fluid. SRX Physics. 2010.

Salleh, M. Z., Nazar, R. & Pop, I. (2010b). Mixed convection boundary layer flow about a solid sphere with Newtonian heating. Archives of Mechanics. 62, 283-303.

Tham, L., Nazar, R. & Pop, I. (2013). Mixed convection flow over a solid sphere embedded in a porous medium filled by a nanofluid containing gyrotactic microorganisms. International Journal of Heat and Mass Transfer. 62, 647-660.

Usman, M., Soomro, F. A., Haq, R. U., Wang, W. & Defterli, O. (2018). Thermal and velocity slip effects on Casson nanofluid flow over an inclined permeable stretching cylinder via collocation method. International Journal of Heat and Mass Transfer. 122, 1255-1263.

Yuge, T. (1960). Experiments on heat transfer from spheres including combined natural and forced convection. Journal of Heat Transfer. 82, 214-220.

Zokri, S. M., Arifin, N. S., Salleh, M. Z., Kasim, A. R. M., Mohammad, N. F. & Yusoff, W. N. S. W. (2017). MHD Jeffrey nanofluid past a stretching sheet with viscous dissipation effect. Journal of Physics: Conference Series. 012002.

Zokri, S. M., Arifin, N. S., Mohamed, M. K. A., Kasim, A. R. M., Mohammad, N. F. & Salleh, M. Z. (2018). Influence of viscous dissipation on the flow and heat transfer of a Jeffrey fluid towards horizontal circular cylinder with free convection: A numerical study. Malaysian Journal of Fundamental and Applied Sciences. 14, 40-47.